Received: 18 November 2016 | Revised: 28 January 2017 | Accepted: 20 March 2017

DOI: 10.1111/cbdd.12987

RESEARCH ARTICLE

WILEY

Reprofiling of full-length phosphonated carbocyclic 2′-oxa-3′-aza-nucleosides toward antiproliferative agents: Synthesis, antiproliferative activity, and molecular docking study

Majdi M. Bkhaitan[1] | **Agha Zeeshan Mirza**[2] | **Ashraf N. Abdalla**[3] | **Hina Shamshad**[1] | **Zaheer Ul-Haq**[4] | **Mohammed Alarjah**[1] | **Anna Piperno**[5]

[1]Department of Pharmaceutical Chemistry, Faculty of Pharmacy, Umm Al-Qura University, Makkah, Saudi Arabia

[2]Science and Technology Unit (STU), Umm Al-Qura University, Makkah, Saudi Arabia

[3]Department of Pharmacology and Toxicology, Faculty of Pharmacy, Umm Al-Qura University, Makkah, Saudi Arabia

[4]Dr. Panjwani Center for Molecular Medicine and Drug Research, International Center for Chemical and Biological Sciences, University of Karachi, Karachi, Pakistan

[5]Department of Chemical, Biological, Pharmaceutical and Environmental Sciences, University of Messina, Messina, Italy

Correspondence
Majdi M. Bkhaitan, Department of Pharmaceutical Chemistry, Faculty of Pharmacy, Umm Al-Qura University, Makkah, Saudi Arabia.
Email: mmbakhaitan@uqu.edu.sa or mmmbk70@gmail.com

Funding information
King Abdulaziz City for Science and Technology, Grant/Award Number: 11-MED 1699-10

A series of phosphonated carbocyclic 2′-oxa-3′-aza-nucleosides were synthesized via 1,3 dipolar cycloaddition and evaluated for their in vitro antiproliferative activity against the growth of cancer cell lines (MCF-7, A2780, HCT116) and normal non-transformed fibroblast (MRC5) using MTT assay. Synthesized compounds exhibited antiproliferative activity in the micromolar range. Compounds 11b showed the highest activity against MCF-7 cells (IC_{50} of 0.2344 μM). Cell cycle analysis was performed for compound 11b on MCF7 cells showing arrest of cells in the S phase. Molecular docking of synthesized compounds confirmed high affinity of these compounds to two different receptors for anticancer nucleosides on dCK, namely the 1P5Z and 2ZIA, showing scores higher than the cognate ligand for all tested compounds. All synthesized compounds were evaluated according to the Lipinski, Veber, and Opera rules, and all of them passed the evaluation showing excellent features, superior to reference drugs. In addition, ADME for all the synthesized compounds was predicted through a theoretical kinetic study using the DISCOVERY STUDIO 3.1 software.

KEYWORDS
ADME, antiproliferative, deoxycytidine kinase, isoxazolidine nucleosides, molecular docking, phosphonated nucleosides

1 | INTRODUCTION

The development of phosphonated nucleosides as new antiviral and anticancer agents is an important area of research. In this context, research has focused on modification of naturally occurring nucleotides at the nucleobase, sugar, and phosphate unit level. Chemical modification of natural nucleoside monophosphates (NMP) to produce phosphonated nucleosides has proved to enhance the activity and generate potent compounds; a-phosphonate is known to be chemically and enzymatically stable as its phosphorous–carbon bond is not susceptible to acidic and phosphatase hydrolysis, in addition to its ability to rely on cellular kinases for further phosphorylation.[1]

Nucleoside phosphonate concept has been applied to design furanose phosphonated nucleosides as well as nucleosides bearing an additional manipulation on the sugar and/or base moieties (i.e., carbocyclic, heterocyclic and acyclic

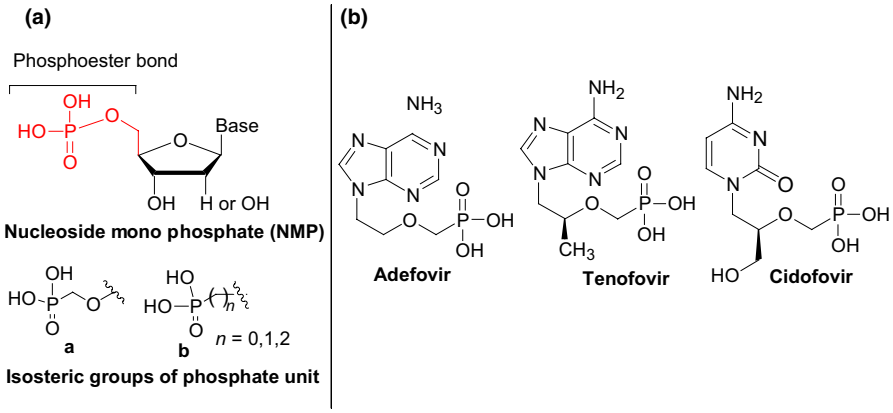

FIGURE 1 (a) Structure of nucleosides and the isosteric groups of the phosphate unit. (b) Examples of FDA-approved phosphonated nucleotides [Colour figure can be viewed at wileyonlinelibrary.com]

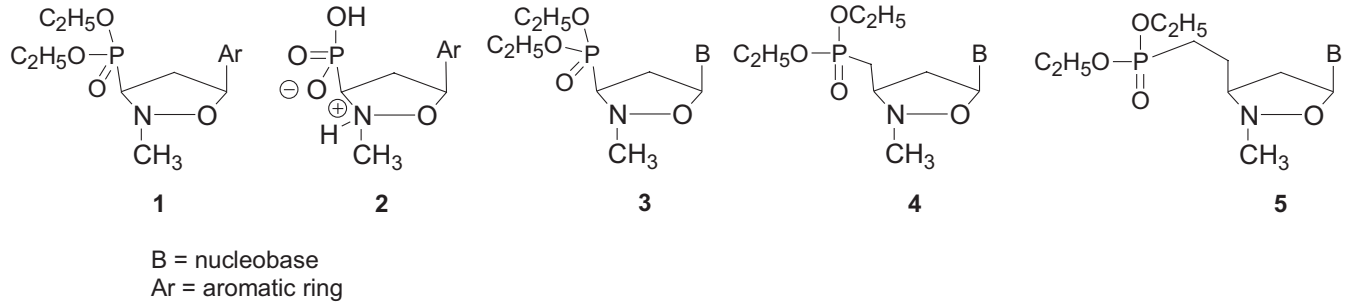

FIGURE 2 Structure of phosphonated isoxazolidine nucleosides

nucleosides).[2–7] This concept has led to the introduction of clinically approved drugs for hepatitis B (adefovir), human immunodeficiency virus (tenofovir), and cytomegalovirus retinitis in patient with AIDS (cidofvir) (Figure 1b).[8,9]

Among the various isosters of the phosphate group (Figure 1a), the "type a" obtained by replacing the 5′-oxygen with carbon gave the best results in the discovery of clinically approved antiviral agents (Figure 1b). The switching maintains the length of natural phospho-ester chain, and the oxygen atom close to the phosphorous atom allows the coordination processes that facilitate the transfer of nucleotidyl group in the polymerase reactions.[4] Relevant biological activities were also discovered in heterocyclic phosphonated nucleosides designed with the "type b" isoster group (Figure 2). In particular, important antiviral and antiproliferative activities were reported for phosphonated isoxazolidine nucleosides **1**, **2**, **3** and **4** containing the nitrogen atom of heterocyclic ring close to the phosphonate unit.

5-arylisoxazolidin-3-diethoxyphosphonates and phosphonates possessing 1- and 2-naphthyl groups at C5 **1** as well as their phosphonic acids **2** have been found to be antiproliferative to HeLa and K562 cells with IC_{50} in the 0.1–0.3 mM range.[10] Isoxazolidine nucleosides **3** and **4** have been extensively explored both as antiviral and antiproliferative agents; they are endowed of important antiviral and antiproliferative properties.[11–13] In particular, from this study emerges a strong ability to inhibit the reverse transcriptase of human T-cell leukemia virus type 1 (HTLV1).[14]

The synthesis of pyrimidinic nucleosides **5** together with their preliminary evaluation against reverse transcriptase was reported in 2006.[15] No antiviral activity was found; thus, the antiproliferative activity has not been investigated and no further development of these compounds was reported till now.

Here, we report the synthesis and antiproliferative activity of phosphonated isoxazolidine nucleosides **11a–d** and **12a–d** (Scheme 1) and their monoesters **13** and **14** (Scheme 2), because we believe that compounds type 5 deserve further investigations due to their structural analogy to natural NMP. In fact, they can act as C-nucleosides where the oxygen atom of the furanose ring is replaced with a carbon atom. In addition, the replacement of P–O–C fragment with a P–C–C unit maintains the same chain length between the nucleobase and phosphorous atom of NMP.[15–17]

Docking studies of the synthesized compounds were carried out using deoxycytidine kinase (dCK) which is considered responsible not only for phosphorylation of several deoxynucleosides but also numerous nucleoside analog prodrugs which are used in cancer and antiviral chemotherapy.[18] Human dCK has two subunits (homodimer) possessing 260 amino acids each,[19] and its crystal structure (1p5z.pdb, 2zia.pdb) clearly shows that pyrimidine- and purine-based inhibitors binding in the active site of dCK are strongly maintained by different types of interactions. It was documented that dCK inhibitors, in combination with other agents that can cause pharmacological perturbations of de novo deoxynucleoside triphosphates (dNTP) biosynthesis, would eliminate acute

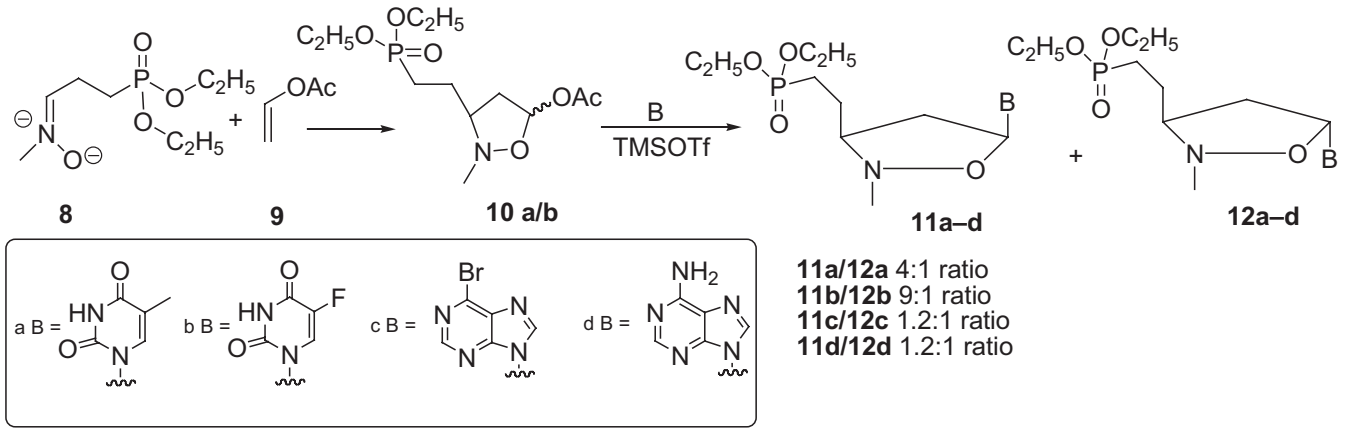

SCHEME 1 Synthesis of Phosphonated carbocyclic 2′-oxa-3′-aza-nucleosides

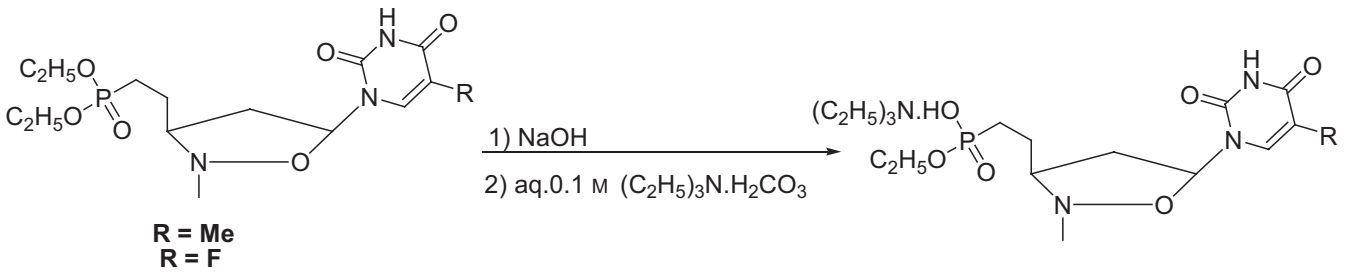

SCHEME 2 Preparation of compounds **13** and **14** through alkaline hydrolysis

lymphoblastic leukemia cells and possibly other cancers in animal models,[20] and its activity is prevalent in most of the solid tumors and its substrate specificity is very broad.[21] These docking studies were conducted to explore whether the interactions of the designed inhibitors were maintained and strengthened further by incorporating a monophosphonate ester group. Druglikeness properties of the synthesized compounds were evaluated using Lipinski's rule of five,[22] Veber rule of bioavailability,[23] and Opera rule[24,25] showing that all compounds pass the three filters successfully. Pharmacokinetic studies (ADME) were also conducted using the DISCOVERY STUDIO 3.1 (DS) software revealing that all synthesized compounds present very good to optimal pharmacokinetic properties which suggest that these derivatives are promising candidates as anticancer agents.

2 | MATERIALS AND METHODS

All solvents and reagents were obtained from Sigma-Aldrich Chemical Co. USA, unless otherwise mentioned and purified before use if necessary. Compounds **8** and **10a/b** were prepared according to reported literature.[15] Thin-layer chromatography was performed using Sigma-Aldrich silica gel 60-F254 pre-coated aluminum plates. IR spectra were performed using Tensor 37 FTIR (Bruker Corporation) by KBr disk method, with OPUS 7.2 software. LCMS analysis was performed using Shimadzu LCMS-2010EV instrument with electrospray ionization (ESI) interface. The ESI source was operated in positive ionization mode for compounds **11** and **12** and negative ionization mode for compound **13** and **14**. HPLC analysis was performed using Shimadzu Prominence LC-20AD liquid chromatography with a diode array detector. Separations were achieved with gradient system elution using a mobile phase composed of 90% water (0.5% trifluoroacetic acid) to 40% water (0.5% trifluoroacetic acid) on Phenomenex Luna C18 (15 mm × 250 mm) column, while 1H NMR spectra using $CDCl_3$ and D_2O as solvents were recorded on Bruker Avance III 300 MHz NMR spectrometer while ^{13}C NMR and ^{31}P-NMR spectra were recorded using $CDCl_3$ and DMSO-*d*6 as solvents on Bruker 500 MHz spectrometer at 125 and 202 MHz, respectively, with TOPSPIN 3.2 software.

2.1 | General chemistry

2.1.1 | General procedure for the preparation of nucleotides 11a–d and 12a–d

Nucleotides **11a–d** and **12a–d** were obtained by modification of procedure previously reported.[15] Briefly, bis(trimethylsilyl)-acetamide (BSA) (1.25 mmol) was added on suspension of nitrogen base (a–d) (0.31 mmol) in dry acetonitrile (3 ml) and refluxed under stirring until the solution

became clear. A solution of the epimeric isoxazolidines **10ab** (0.25 mmol) in dry acetonitrile (3 ml) and trimethylsilyltriflate (TMSOTf) (0.4 mmol) was added, and the reaction mixture was stirred at 55°C for 6 hr. After being cooled at 0°C, the solution was brought to neutrality by adding an aqueous 5% sodium bicarbonate, concentrated in vacuo, and extracted with dichloromethane. The organic phase was dried over sodium sulfate, filtered, and evaporated to dryness. The residue was purified by column chromatography using $CHCl_3$/CH_3OH (99:1) as eluent.

Diethyl{(1′SR,4′RS)-1′-[[5-methyl-2,4-dioxo-3,4-dihydropyrimidin-1(2H)-yl]-3′-methyl-2′-oxa-3′-azacyclopent-4′-yl]}ethylphosphonate (**11a**). Pale yellow gum (40% yield), data of the NMR spectra matched those reported in the literature.[15]

Diethyl[(1′SR,4′RS)-1′-(5-fluoro-2,4-dioxo-3,4-dihydropyrimidin-1(2H)-yl)-3′-methyl-2′-oxa-3′-azacyclopent-4′-yl] ethylphosphonate (**11b**), white solid (53% yield), NMR spectra matched those reported in the literature.[15]

The reaction of **10ab** with adenine afforded the mixture of diethyl 2-[(3RS,5SR)-5-(6-amino-9H-purin-9-yl)-2-methylisoxazolidin-3-yl] ethylphosphonate (**11c**) and diethyl 2-[(3RS,5RS)-5-(6-amino-9H-purin-9-yl)-2-methylisoxazolidin-3-yl] ethylphosphonate (**12c**). Compounds **11c** and **12c** were isolated as diastereomeric mixture, global yield 56%, solubility: >10 mg/ml in DMSO, <1 mg/ml in water, IR (KBr): 3,396, 1,447, 1,601, 1,260, 1,216, 1,024, 968 cm^{-1}, 1H NMR: δH (300 MHz, $CDCl_3$): β isomer 1.25–130 (t, 6H, $J = 7.5$ Hz), 1.65 (m, 2H), 1.90 (m, 2H), 2.33 (ddd, 1H, $J = 3.0$; 9.0 and 13.5 Hz), 2.58 (m, 1H), 2.73 (s, 3H), 3.08 (m, 1H), 4.05 (q, 4H, $J = 7.5$ Hz), 5.61 (sb, 2H), 6.33 (dd, 1H, $J = 3.0$ and 5.4 Hz), 7.96 (s, 1H), 8.15 (s, 1H). α-isomer, 1.25–130 (m, 6H, $J = 7.5$ Hz), 1.65 (m, 2H), 1.95 (m, 2H), 2.77 (s, 3H), 2.78 (m, 1H), 3.03 (m, 1H), 3.24 (m, 1H), 4.05 (q, 4H, $J = 7.5$ Hz), 5.61 (s, 2H), 6.21 (dd,1H, $J = 3.5$ and 9.0 Hz), 8.27 (s, 1H), 8.28 (s, 1H). mixture of α- β isomers 13C NMR: δC (125 MHz, $CDCl_3$): 16.74, 16.79, 22.45, 24.30, 43.58, 43.65, 61.48, 61.58, 68.36, 68.50, 80.05, 82.13, 119.03, 119.52, 139.23, 139.77, 149.73, 149.83, 153.09, 153.18, 156.44.156.50, ^{31}P-NMR: δ (202 MHz, DMSO-*d*6): 31.22, EI MS (m/z): 384.90 [MH+]; cld for C15H25N6O4P: 384.167.

The reaction of **10ab** with 6-bromopurine afforded the mixture of diethyl 2-[(3RS, 5SR)-5-(6-bromo-9H-purin-9-yl)-2-methylisoxazolidin-3-yl]ethylphosphonate (**11d**) and diethyl2-[(3RS,5RS)-5-(6-bromo-9H-purin-9-yl)-2-methylisoxazolidin-3-yl] ethylphosphonate (**12d**). Pale yellow gum (global yield 45%), molecular weight 448.26, solubility: >10 mg/ml in DMSO, <1 mg/ml in water, IR (KBr): 3,417, 2,984, 1,635, 1,587, 1,560, 1,394, 1,250, 1,215, 1,052, 1,024, 968 cm^{-1}. 1H NMR: δH (300 MHz, $CDCl_3$): β isomer, 1.20 (t, 6H, $J = 7.3$ Hz), 1.68 (m, 2H), 1.94 (m, 2H), 2.35 (ddd, 1H, $J = 3.0$; 9.2 and 12.3 Hz), 2.59 (m, 1H), 2.77 (s, 3H), 3.25 (m, 1H), 4.12 (q, 4H, $J = 7.3$ Hz), 6.36 (dd, 1H, $J = 3.0$ and 6.2 Hz), 7.30 (s, 1H), 8.47 (s, 1H). α-isomer, 1.20 (m, 6H, $J = 7.3$ Hz), 1.68 (m, 2H), 1.94 (m, 2H), 2.75 (s, 3H), 2.76 (m, 1H), 3.02 (m, 1H), 3.35 (m, 1H), 4.12 (q, 4H, $J = 7.3$ Hz), 6.25 (dd,1H, $J = 3.0$ and 8.5 Hz), 8.61 (s, 1H), 8.64 (s, 1H). mixture of α- β isomers 13C NMR: δC (125 MHz, $CDCl_3$): 16.66, 16.72, 23.79, 24.11, 43.15, 43.48, 46.13, 46.31, 61.53, 61.78, 69.63, 82.13, 119.52, 140.46, 145.91, 146.50, 148.21, 149.67, 152.03, 152.16, 155.46, ^{31}P-NMR: δ (202 MHz, DMSO-*d*6): 31.48, EI MS (m/z): 447.8 [MH+]; cld for C15H23BrN5O4P 447.067.

2.1.2 | Preparation of compounds phosphonic acid monoethyl ester 13 and 14

The diethyl ester **11a** or **11b** (1.25 mmol) was dissolved in tetrahydrofuran and was hydrolyzed to the monoethyl ester by reaction with 10 mole equivalents of 3 M sodium hydroxide overnight. The crude product was purified by automated reversed-phase chromatography using a gradient of 0%–100% aqueous 0.1 M triethylammonium carbonate (pH 8) with the balance being acetonitrile producing **13** and **14**.

Triethylamine ethyl l2-[(3R,5S)-2-methyl-5-(5-methyl-2,6-dioxo-1,2,3,6-tetrahydropyridin-3-yl) isoxazolidin-3-yl] ethylphosphonate (**13**); white solid (35% yield), mp. 117°C (bubbles). Solubility: >10 mg/ml in DMSO, >10 mg/ml in water. IR (KBr): 3,422, 2,975, 2,803, 2,491, 1923, 1,700, 1,480, 1,278, 1,159, 1,035, 946, 834, 814, 763, 702 cm^{-1}. 1H NMR: δH (300 MHz, D2O): 1.14 (t, 9H, $J = 6.0$ Hz), 1.52 (t, 3H, $J = 6.6$ Hz), 1.51 (m, 3H), 1.75 (m, 1H), 1.76 (d, 3H, $J = 0.8$ Hz), 2.07 (s, 1H), 2.68 (s, 3H), 2.70 (s, 1H), 3.0 (s, 1H), 3.08 (q, 6H, $J = 6.0$ Hz), 3.79 (q, 2H, $J = 6.6$ Hz), 6.07 (dd,1, $J = 6.0$ and 9.1 Hz),7.58 (q, 1H, $J = 0.8$ Hz). 13C NMR: δC (125 MHz, D_2O): 12.16, 12.56, 17.53, 17.58, 24.39, 43.07, 43.62, 46.15, 58.42, 69.61, 81.64, 109.56, 136.73, 151.0, 164.32, 31P-NMR: δ (202 MHz, DMSO-d6): 18.95, EI MS (m/z): 345.95 [MH–]; cld for C13H22N3O6P 347.125.

Triethylamine ethyl 2-((3R,5S)-5-(5-fluoro-2,6-dioxo-1,2,3,6-tetrahydropyridin-3-yl) -2-methylisoxazolidin-3-yl) ethylphosphonate (**14**). white solid (38% yield), solubility >10 mg/ml in DMSO, >10 mg/ml in water, M.P. 101°C (bubbles), IR (KBr): 3,406, 2,979, 2,844, 1920, 1,706, 1,562, 1,401, 1,259, 1,152, 1,057, 941, 883, 814, 708 cm^{-1}, 1H NMR: δH (300 MHz, D_2O): 1.15 (t, 9H, $J = 6.1$ Hz), 1.53 (t, 3H, $J = 6.7$ Hz), 1.50 (m, 3H), 1.77 (m, 1H), 2.03 (s, 1H), 2.67 (s, 3H), 2.72 (s, 1H), 3.02 (s, 1H), 3.10 (q, 6H, $J = 6.7$ Hz), 3.75 (q, 2H, $J = 6.7$ Hz), 6.01 (dd,1H, $J = 5.7$ and 8.9 Hz), 7.89 (d, 1H, $J = 7.1$ Hz). 13C NMR: δC (125 MHz, D_2O): 12.15 (CH_3–CH_2–N), 17.53 (CH_2–CH_2–PO), 17.57 ($POCH_2$–CH_3), 23.99 (CH_2–CH_2–PO), 43.27 (CH_3 group attached with isoxa), 43.48 (O–HC–C, isoxa), 46.15 (CH_3–CH_2–N),

58.41 ($POOCH_2$), 69.42 (N–CH, isoxa), 82.26 (O–HC–C, isoxa), 124.68 (=C–NH, base), 141.43 (FC=CH, base), 148.78 (N–CO–NH, base), 156.99 (OC–N, base), ^{31}P-NMR: δ (202 MHz, DMSO-*d*6): 18.92, EI MS (m/z): 349.95 [MH-]; cld for C12H19FN3O6P 351.099.

2.2 | Cell culture

MCF7 (human breast adenocarcinoma), A2780 (human ovarian cancer), HCT116 (human colorectal carcinoma), and MRC5 (normal non-transformed fibroblast) cell lines were purchased from ATCC and were cultured in flasks which were kept incubated at 37°C in an atmosphere of 5% CO_2, 95% air, and 100% relative humidity, to maintain continuous logarithmic growth. RPMI-1640 media were supplemented with 10% heat-inactivated fetal bovine serum (FBS), L-glutamine, and 1% penicillin/streptomycin. Cells were used within 20 passages (except for MRC5: five passages) and were checked for mycoplasma every 6 months by measuring the bioluminescence (Myco Alert sample detection kit; Lonza, Switzerland) using a multiplate reader (Synergy HT, BioTek, USA).

2.3 | MTT cell proliferation assay

The MTT in vitro cell viability colorimetric assay was used for measuring cellular proliferation and inhibitory activity[26] of the synthesized compounds.

3-(4,5-Dimethylthiazol-2-yl)-2,5-diphenyltetrazolium bromide: MTT is a yellow tetrazole which is reduced to formazan (purple) when mitochondrial dehydrogenase enzymes are active, and therefore, reduction indicates cell viability, which can be measured as optical density (OD). Cells from flasks of 70%–80% confluences were separately seeded in 96-well flat-bottomed microculture plates (Nalgene-Nunc, Thermo Fisher Scientific, Denmark) at density of 3×10^3 cells (MCF7, A2780 and MRC5) and 10×10^3 cells (HCT116), to a volume of 180 µl/well of culture medium. Cells were counted and incubated at 37°C overnight to allow attachment to the wells. Final concentrations of each compound in wells were as follows: 0.0, 0.005, 0.05, 0.5, 5, 25, 50, and 100 µM/ml in 200 µl of media (DMSO 0.1% v/v). 5FU was used as positive control at the same final concentrations. Medium only (20 µl) was added to each control well, and each concentration was tested in triplicates ($n = 3$). Following incubation for 72 hr, 50 µl MTT was added into each well. Plates were incubated for 3 hr, the supernatant was aspirated, and 100 µl of DMSO was added to each well. Plates were shaken for 5 min at 26°C using STUART scientific orbital shaker (Redhill, Surrey, UK) and absorbance read on the multiplate reader. The optical density of the purple formazan A_{550} is proportional to the number of viable cells. When the amount of formazan produced by treated cells is compared with the amount of formazan produced by untreated control cells, the strength of the drug in causing growth inhibition can be determined, through plotting growth curves of absorbance against drug concentration; thus, formulation concentration causing 50% inhibition (IC_{50}) compared to control cell growth (100%) was determined. GRAPHPAD Software, San Diego, California, was used for analysis.

2.4 | Perturbation of cell cycle analysis

The cell cycle is a series of changes occurring from the initial phase of cell formation leading to its division as a consequence of a specific mechanism. Cell cycle phases include G_1 (gap 1), S (synthesis), G_2 (gap 2), and M (mitosis), with cell cycle arrest usually taking place in the G_1/S or the G_2/M checkpoints. Disruption of cell cycle causes cancer. Cell cycle distribution analysis was performed based on a previously described method.[27] Propidium iodide (PI) fluorescence-labeled cell nuclei were suspended in a stream of fluid, and an argon laser $A_{488/645}$ was used to excite PI (emission A_{617}), and emission above A_{550} was collected. MCF7 cells were seeded in six-well plates at 1×10^5 cells/well in 2 ml medium and were left to attach overnight, before treatment with control or drug 2 ($n = 2$) to final concentrations: 0, 1, 5, and 10 µM. Then, plates were incubated for 72 hr. After incubation, the medium was collected and kept on ice. Cells were washed with ice-cold PBS (2×). Trypsin (0.5 ml) was added to each well and incubated at 37°C for 5 min; detached cells were pooled with the floating cell suspension. Then, tubes were centrifuged at 210 g for 5 min at 4°C and the supernatant discarded. Pellets were washed with 1 ml of PBS, centrifuged, and fixed for 2 hr in 70% ice-cold ethanol. Then, pellet was centrifuged, re-suspended in PBS with the addition of ribonuclease A (15 min), followed by PI (2 µl/ml). Samples were held on ice and analyzed by flow cytometry (BC FC500). Data analysis of DNA contents (PI bound to DNA) of 20,000 events was carried out using EXPO 32 software. Doublets were differentiated from single cells in the G_2/M phase by gating them out manually.

2.5 | Molecular docking

Molecular docking studies were carried out on the inhibitors to generate the bioactive conformation within the binding site of the protein and to understand the binding interactions through DISCOVERY STUDIO 3.1 (Accelrys Inc., USA, 2013) using LIBDOCK Tool. Ligands after preparation from ChemDraw were imported in the DS and prepared using "Prepare ligands" tool in DS. The default parameters were used for ligand preparation using ionization based on pH method. The prepared compounds were fully minimized using Charm M forcefield method. 1P5Z.pdb and 2ZIA.pdb were retrieved from Brookhaven Protein Data Bank (PDB),

USA (http://www.rcsb.org/pdb), which is a repository of experimentally determined crystal structures of macromolecules. Receptors of the selected proteins were created using "prepare protein" tool in DS and typed using the CharmM force field. The binding site was defined by co-crystallized cognate ligand as cytarabine in the case of 1P5Z.pdb and cladribine for 2ZIA.pdb. Redocking studies were carried out by generating a sphere of hot spots (100) in the active site using the fast conformational method with docking tolerance of 0.25. LIBDOCK score was used to rank the ligand poses, and in situ minimization was performed on top poses of the two receptors to optimize the docked pose. 2D and 3D diagrams were generated which further depicted interaction pattern. To study the differences in the binding sites, 1P5Z.pdb and 2ZIA.pdb were aligned and superimposed using "Align and Superimpose" tool in macromolecule window having 1P5Z. pdb as reference protein in the first instance and then making 2ZIA.pdb as a reference in the second instance. Docked compounds of one protein were then inserted and visualized in the binding cavity of other protein.

2.6 | ADME and druglikeness

The drug-like properties and ADME of the prepared and minimized compounds were evaluated using DS 3.1. Druglike properties were assessed using three filters as Lipinski's rule of five.[22] Veber rule of bioavailability[23] and Opera rule.[24,25] For ADME studies, the aqueous solubility, blood–brain barrier penetration (BBB), cytochrome P450 2D6 binding (CYP2D6), intestinal absorption (HIA), and plasma protein binding (PPB) were calculated. These properties were helpful to ascertain the failure or success of these novel candidates and are now an essential part of drug designing processes.[22]

3 | RESULTS AND DISCUSSION

3.1 | Chemistry

Phosphonated carbocyclic 2′-oxa-3′-aza-nucleosides **11a–d** and **12a–d** were synthesized by a two-step procedure, starting from phosphonated nitrone **8**, and according to literature method.[15] The two-step methodology is based on the 1,3-dipolar cycloaddition of phosphonated nitrone **8** with vinyl acetate **9** to obtain cycloadducts **10a/b**, followed by Vorbrüggen nucleosidation (Scheme 1).

The nucleosidation reactions with pyrimidine bases were performed using silylated thymine and silylated 5-fluorouracil in acetonitrile at 55°C in the presence of 0.4 equiv. of trimethylsilyltriflate (TMSOTf) as a catalyst. In agreement with what reported in literature, β-anomers **11a** and **11b** were obtained as main isomers and in good yields. The synthetic methodology was also applied to the preparation of new adenine and 6-bromopurine derivatives. The nucleosidation reactions with purine bases afforded nearly equimolecular mixtures of inseparable α- and β-nucleosides (α/β ratio = 1:1.2 ratio). The molecular structure of the reaction products was assigned on the basis of analytical data, spectroscopic data, and NOE measurements. In particular for compound **11c**, one- and two-dimensional NMR data revealed that the signals at 2.33 ppm (ddd, H4′a), 2.58 ppm (m, H′-4b), 2.73 ppm (s, N–CH_3), 3.08 (m, H′-3), 6.33 ppm (dd, H′-5), 7.96 ppm (s, H-3), 8.15 ppm (m, H-8) can be attributed to the β-diastereomer. The cross-peaks in 2D-NOESY spectrum between the signal at 6.33 ppm (H′-5), 2.33 ppm (H4a′), and 3.08 (m, H′-3) are indicative of the cis configuration between nucleobase and $CH_2CH_2P(O)(OEt)_2$.

The stereochemical experimental outcomes of the nucleosidation reactions were in satisfactory agreement with literature data.[12]

The antiproliferative activity of pyrimidine β-isomers (**11a** and **11b**) and of purine nucleosides as anomeric mixtures (**11c/12c** and **11d/12d**) was evaluated in vitro against different tumor cell lines. Moreover, considering that phosphonated nucleosides can be further phosphorylated in vivo, the monoester of thymine and 5-fluorouracil derivatives were synthesized under alkaline hydrolysis conditions.[28,29]

The very clean products **13** and **14** were obtained through the controlled hydrolysis of **11a** and **11b** using sodium hydroxide, and then, the crude product obtained was purified by automated reversed-phase chromatography using a gradient of 0%–100% aqueous 0.1 M triethylammonium carbonate (Scheme 2). The structures of **13** and **14** were fully confirmed by instrumental analysis ^{1}H, ^{13}C, ^{31}P-NMR, IR, and mass spectra.

In contrast to the pyrimidine derivatives, the hydrolysis of the purine diesters to their corresponding monoesters has proved to be extremely difficult. The bromopurine derivative gives none of the desired product and evidence indicates that the bromine displacement takes place before ester hydrolysis. In hydrolysis experiments with adenine diester derivative, the presence of some monoesters can be detected forcing the reaction conditions but under these experimental conditions, significant cleavage of the purine ring occurs.

3.2 | Antiproliferative activity

The synthesized compounds were evaluated for their antiproliferative properties in vitro on human breast adenocarcinoma (MCF7), human ovarian cancer (A2780), human colorectal carcinoma (HCT116), and normal non-transformed fibroblast (MRC5) cell lines using MTT cell proliferation assay;[26] 5-fluoruracil (5-FU) was used as reference (Table 1).

All prepared compounds showed antiproliferative activity in the micromolar range, and in particular, compounds **13**, **14**, and **11a** showed higher potency against HCT116

TABLE 1 Antiproliferative activity (μM, $IC_{50} \pm SD$, 72 hr) of the compounds and 5-FU against MCF7, A2780, HCT116, and MRC5 cell lines

Compounds	MCF7	A2780	HCT116	MRC5
11a	45.75 ± 3.18	12.58 ± 3.41	1.86 ± 0.08	0.20 ± 0.01
11b	0.23 ± 0.09	2.72 ± 0.67	17.74 ± 0.36	0.76 ± 0.04
11c/ 12c	25.53 ± 2.07	0.32 ± 0.13	>100	9.62 ± 3.09
11d/12d	2.55 ± 0.99	18.40 ± 2.26	10.58 ± 0.73	0.15 ± 0.01
13	10.61 ± 0.36	15.09 ± 1.28	0.275 ± 0.07	1.39 ± 0.13
14	29.86 ± 1.60	59.22 ± 1.09	0.685 ± 0.02	1.20 ± 0.41
5FU	19.21 ± 0.56	4.80 ± 0.36	2.72 ± 0.90	2.70 ± 0.20

Data shown in mean ± *SD*. Experiment was repeated 3× independently.

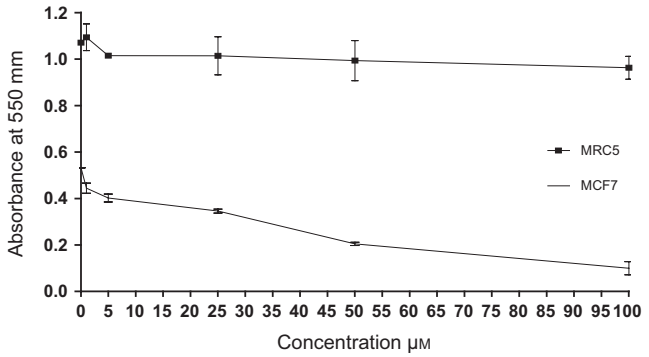

FIGURE 3 Antiproliferative activity of 11b (MTT 72 hr) against MRC5 and MCF7 cell growth

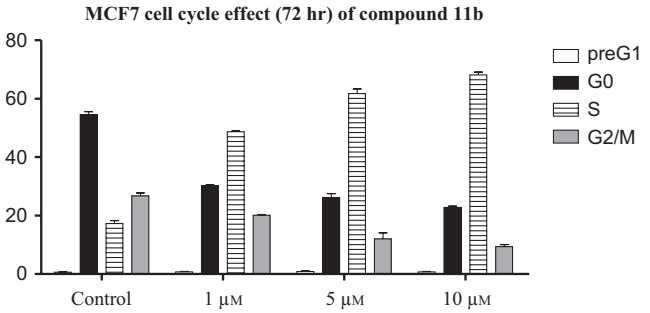

FIGURE 4 Cell cycle phases of MCF7 treated with compound **11b**: (72 hr, *x*-axis); % cell number: *y*-axis. Data shown in mean % ± *SD* ($n = 3$). Experiment was repeated 3×

cell lines than 5-FU (ten-, four-, and twofold, respectively). Compound **11b** showed good activity in all cell lines and in particular against MCF7 cell lines (80 folds more potent than the reference drug) (Figure 3).

Compound **11d/12d** as isomeric mixture exhibited its highest activity against MCF7 cells. Interestingly, compound **11/12c** as isomeric mixture was highly potent against A2780 cells, being 15-fold more potent than the reference drug. The IC_{50} of the reference drug (5-FU) against MRC5 was 2.72 μM, showing no selectivity compared to cancer cells and demonstrating high toxicity. Compound **11/12c** was the least toxic to MRC5 cells, with IC_{50} 9.62 μM (threefold the IC_{50} of 5-FU). The remaining derivatives were more toxic against MRC5 than the reference drug although displaying more activity against specific cancer cell lines.

3.3 | Determination of cell cycle perturbations

Affecting cell cycle phases is a valid cancer therapy target, and many antiproliferative agents produce their antiproliferative effect by causing the arrest of cell cycle at a specific stage.[27,30] Therefore, in order to establish whether the antiproliferative effect of our compounds was due to cell cycle arrest, cell cycle analysis was performed to test the effect of compound **11b** in MCF7 cells (Figure 4).

Compound **11b** was selected because it possessed good antiproliferative activity in all cell lines. MCF7 cells treated with 1 μM showed an increase in S phase compared to control; this accumulation in S phase continued in the higher doses (5 and 10 μM), all at the expense of other stages.

The result indicates that compound **11b** produced S phase arrest in MCF7 cells in a dose-dependent manner, and stopped DNA replication (2–4 folds). This finding demonstrates that synthesized compounds may target rapidly proliferating cells, such as cancer cells (cell cycle diagrams are found in supplementary information).

3.4 | Docking studies

1P5Z.pdb and 2ZIA.pdb structures of dCK having a resolution of 1.6 and 1.8 were retrieved from protein data bank (http://www.rcsb.org/pdb) for docking studies. 1P5Z.pdb and 2ZIA.pdb are co-crystallized with pyrimidine (cytarabine) and purine (cladirabine) base cognates at the acceptor site, whereas adenosine diphosphate and uridine diphosphate at the donor site, respectively. It has been reported that water near Y86 is important for its side-chain positioning and for enzyme selection of open and close state.[31] Hence, the interactions of the docked compounds were studied by keeping 416 (1P5Z.pdb) and 521 (2ZIA) water molecules in the active site of 1P5Z.pdb and 2ZIA.pdb, respectively.

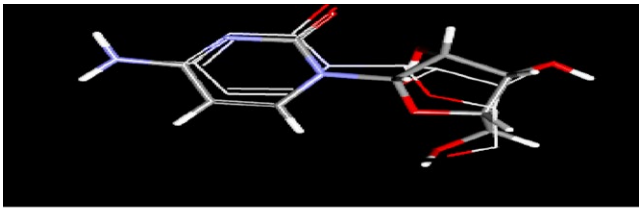

(a) Redocking of cytarabine with water (416)

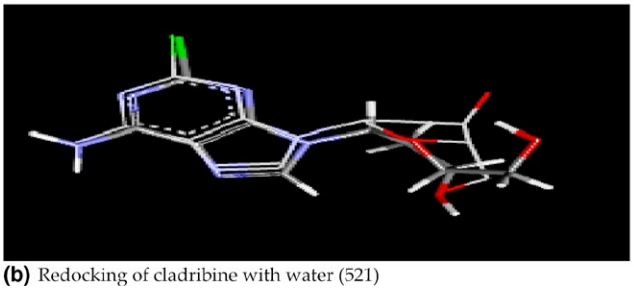

(b) Redocking of cladribine with water (521)

FIGURE 5 Superposition of cognate ligand (molecule displayed in line style) on top scored docked pose (molecule displayed in stick style). (a) 1P5Z.pdb binding site, (b) 2ZIA.pdb binding site. [Colour figure can be viewed at wileyonlinelibrary.com]

Redocking studies were performed on selected dCK proteins to evaluate the performance of the docking software, and RMSD was evaluated from the highest scored docked pose versus cognate ligand extracted from the crystal structure; 0.97 and 1.50 were the RMSD of the top scored pose versus cognate for 1P5Z.pdb and 2ZIA.pdb, respectively (Figure 5a-b).

The same parameters were used to dock inhibitors to the receptors, and comparison was made by evaluating the score and interactions with that of the cognate ligand. Molecular docking studies showed that all compounds consisting of nucleoside phosphonate ester groups were well placed in the active site and showed noticeable interactions (electrostatic, van der Waals, hydrophobic) with the conserved residues, hence ranked above cognates in both proteins.

It was observed that **11b** (most potent experimentally) establishes a number of hydrogen bonds with conserved residues as P loop residue R104, catalytic residue R128, and transition state residue R194[18] as shown in Figure 6a. Moreover, Syn conformation of **11b** facilitated the formation of a hydrogen bond with a water molecule (Figure 6a) while G53 is in a position to compete with R104 for interaction with fluorine. Furthermore, G53 is also lying near to the nitrogen of isoxazolidine and carbon of phosphonate ester.

Pi-pi stacking of fluorouracil ring with F137 from one side is observed while W58 and Phe96 surround it from the other side (Figure 6b-c). I30 establishes polar and hydrophobic contacts with isoxazolidine ring and with carbon C6′ adjacent to isoxazolidine ring. Hydrophobic contacts of V55 and L82 are observed with carbons (C1′ and C5′) of the isoxazolidine ring. V55 is also in a position to form hydrophobic contacts with carbon (C6′) adjacent to isoxazolidine and with one of the ester carbon adjacent to phosphonate (Figure 6b-c). K34 forms polar interaction with isoxazolidine ring and hydrophobic interactions with methyl at isoxazolidine ring and with other ester carbon adjacent to phosphonate. Q97, a conserved residue,[18] establishes polar contact with both oxygen atoms of fluorouracil ring. E127 and S35 are also very close to the oxygen of the ester group of phosphonate. The pattern of binding for all the other compounds in 1P5Z.pdb was almost the same as that of **11b** except for few polar and hydrophobic interactions were lost.

By looking at the **11b** in 2ZIA.pdb, the number of hydrogen bonds with conserved residues and water molecule was observed as shown in Figure 6d. The orientation of the compound was in such a way that R104 and E53 may induce polar interactions. Hydrophobic and polar interactions remained almost the same as in 1P5Z.pdb.

A new interaction with R192 was observed in the binding cavity of 2ZIA.pdb which was absent in 1p5z.pdb as shown in Figure 6e–f. The pattern of binding in the remaining compounds in 2ZIA.pdb was more or less the same as in the case of 1P5Z.pdb losing few of the hydrophobic and polar interactions that were seen with **11b**.

It was observed that in both proteins, the binding pattern of compound **13** was almost the same of **11b**; however, it lost few of the hydrophobic interactions observed in **11b**. In case of compound **14**, we observe the loss of some of the hydrogen bonds and hydrophobic interactions observed in compound **11b** indicating that the freed hydroxyl group did not play a role in increasing the interaction forces with the two proteins.

Docking studies on both the proteins indicated that the presence of phosphonate esters resulted in tighter binding in the acceptor region. These esters were also in position to interact with the donor binding site of the receptor. Furthermore, the presence of isoxazolidine ring in **11b** was found to be involved in polar and hydrophobic interactions with the surrounding residues replacing adequately the natural deoxy sugar. Fluorine found in compound **11b** seems to play a significant role in increasing the affinity with the receptor through the establishment of hydrogen bonding with the charged residues. It is pertinent to mention that the differences in interaction pattern of the compounds within two receptors were observed because of the differences in the side-chain residues of the active site (supplementary information).

3.5 | ADME and druglikeness

Following the promising docking results, all compounds were further subjected to the study of drug-like and pharmacokinetic properties to confirm that all of them follow the standard ranges. Drug-like properties were evaluated using Lipinski's rule of five,[22] Veber rule of bioavailability,[23]

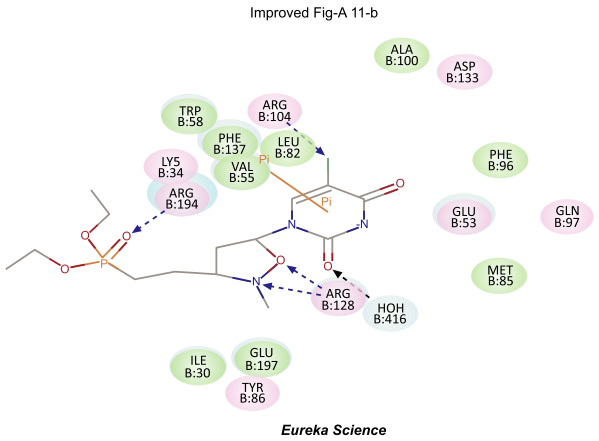

(a) 11b in active site of 1P5Z.pdb

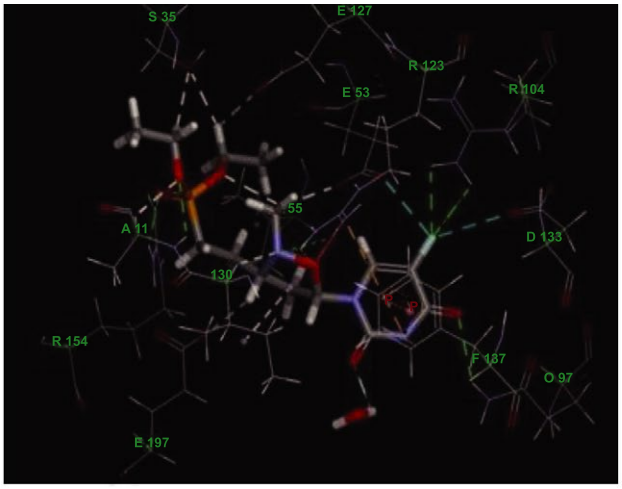

(b) 11b in active site of 1P5Z.pdb

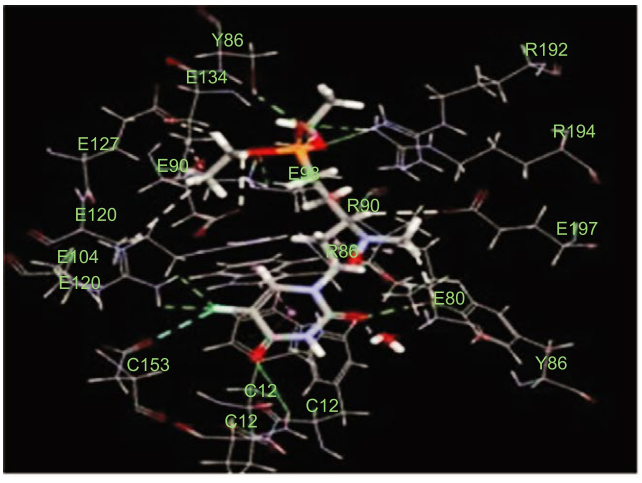

(c) 11b in active site of 2ZIA.pdb

Eureka-Science-D 11b in active site of 2ZIA.pdb

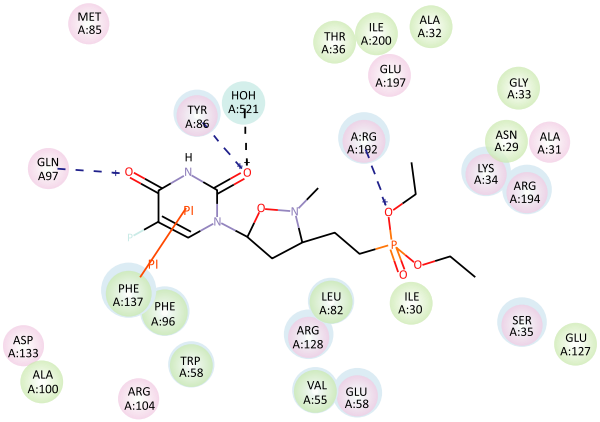

(d) 11b in active site of 2ZIA.pdb

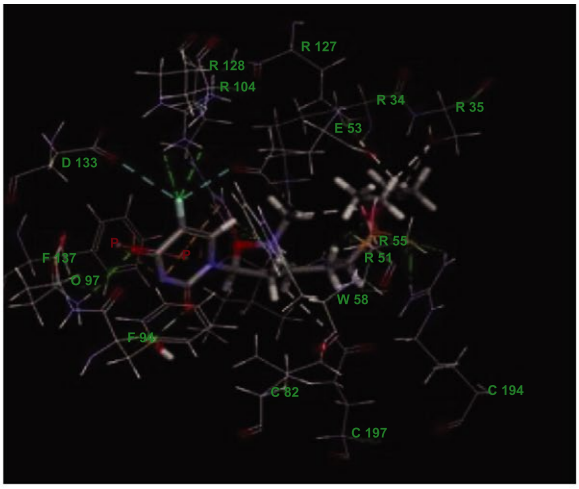

(e) 11b in active site of 1P5Z.pdb

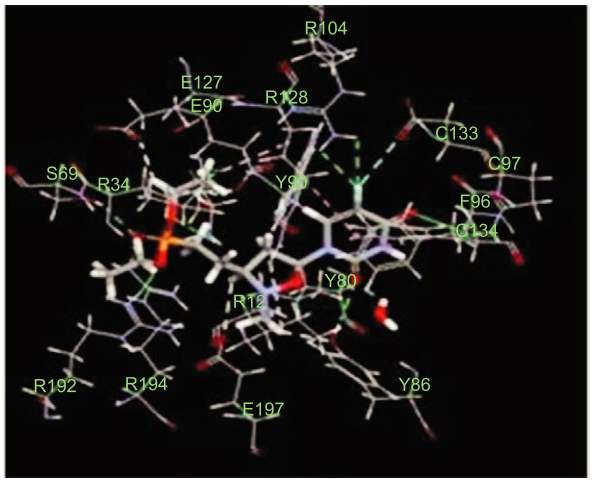

(f) 11b in active site of 2ZIA.pdb

FIGURE 6 (a, b, d) 2D picture of 11b in the active site of two proteins as pink-circled residues indicated hydrogen, charge or polar bonding. Green residues and magenta-colored residues showing van der Waals interaction and covalent bonding. Blue halo indicate solvent-accessible region of the interacting residue. Blue dashed arrow indicates hydrogen bond interactions with side chain of amino acid with direction in both cases toward electron donor, and orange line shows Pi interactions. (b, c, e, f) 3D interaction picture of 11b in the active site [Colour figure can be viewed at wileyonlinelibrary.com]

TABLE 2 Druglikeness of the compounds

Compounds	ALogP	MW	NHA	NHD	NRB	NR	NAR	PSA
11c/12c	−0.277	384.371	9	1	8	3	2	113.114
11d/12d	0.913	448.252	8	0	8	3	2	86.574
11b	−0.833	378.313	7	0	8	2	0	85.397
14	−2.695	349.252	7	0	6	2	0	93.768
13	−2.262	346.296	7	1	6	2	0	106.578
11a	−0.4	375.357	7	1	8	2	0	98.207
Cytarabine	−2.396	243.217	7	4	2	2	0	129.893
Cladribine	−0.259	285.687	7	3	2	3	2	116.232

MW, molecular weight; NHA, number of hydrogen bonds acceptors; NHD, number of hydrogen bond donors; NRB, number of rotatable bonds; NR, number of rings; NAR, number of aromatic rings; PSA, polar surface area.

TABLE 3 ADME of the docked compounds

Name	S levels	BBB levels	CYP2D6	HIA levels	PPB	AlogP98
11c/12c	3	4	FALSE	0	FALSE	0.345
11d/12d	3	3	FALSE	0	FALSE	1.535
11b	4	3	FALSE	0	FALSE	0.439
14	4	3	FALSE	0	FALSE	−0.838
13	4	4	FALSE	0	FALSE	−0.722
11a	3	3	FALSE	0	FALSE	0.556
Cytarabine	5	4	FALSE	3	FALSE	−2.396
Cladribine	4	4	FALSE	0	FALSE	−0.399

S = solubility levels = 0 extremely low, 1 no very low but possible, 2 yes low, 3 yes good, 4 yes optimal, 5 no too soluble. BBB = blood–brain barrier levels = 0 very high, 1 high, 2 medium, 3 low, 4 undefined. CYP2D6 = cytochrome 450 inhibition. HIA = human intestinal absorption levels = 0 good, 1 moderate, 2 poor, 3 very poor. PPB = plasma protein binding. AlogP98 = partition coefficient of octanol/water system.

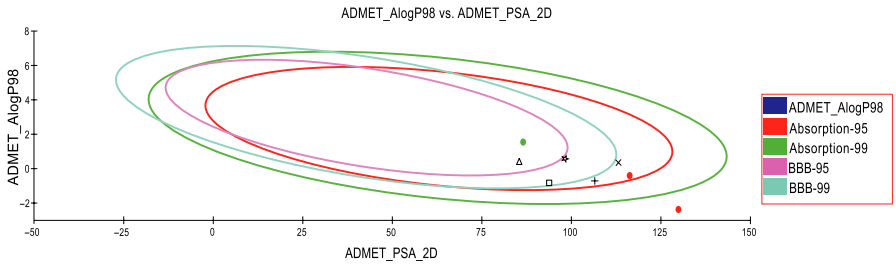

FIGURE 7 Biplot of PSA and AlogP98 showing 95% and 99% ellipses of BBB and HIA. Triangle = 11b, green circle = 12d, purple circle = 11d, star = 11a, X = 12c and 11c, square = 14 and + = 13, two red circles = reference compounds [Colour figure can be viewed at wileyonlinelibrary.com]

and Opera rule.[24] Cytarabine and cladribine were used as a reference for comparison with our compounds. It was observed that only one violation with regard to Oprea (two violations are allowed) of **11c** and **12c** was observed having a number of hydrogen bond acceptors to be nine. Hence, it can be concluded that all compounds pass the three filters successfully as shown in Table 2.

The number of aromatic rings was found to be not more than three which is compatible with druglikeness requirement for anticancer drugs.[32] ADME studies showed very good (level 3) to optimal (level 4) solubility levels, whereas cytarabine showed excessive solubility (level 5) as shown in Table 3. The two variables 95% and 99% confidence ellipses for HIA and BBB based on PSA and AlogP98 are shown in Figure 7.

4 | CONCLUSION

All synthesized compounds presented antiproliferative activity in the micromolar range in at least one of the cell lines, especially compound **11b** which has shown good activity in all cell lines. Cell cycle perturbation was conducted using compound **11b** on MCF7 cells showing that it acts through

inhibition of S phase suggesting that these compounds may target rapidly proliferating cells.

Molecular docking confirmed a high affinity to two different receptors for anticancer nucleosides on dCK, namely the 1P5Z.pdb and 2ZIA.pdb, showing scores higher than the cognate ligand for all tested compounds suggesting that their action may involve dCK inhibition. These results clearly showed tighter binding due to the presence of phosphonate ester while presence of isoxazolidine ring and fluorine in **11b** further complements the interaction with the protein residues. According to the Lipinski, Veber, and Opera rules, all of them passed the evaluation showing excellent features, superior to reference drugs. In addition, ADME for all the synthesized compounds was predicted through a theoretical kinetic study.

The results of our research indicate that these compounds represent valid candidates for further development as anticancer agents. Plans are now to further elucidate the structural requirements for more potent and selective anticancer activity and determine the extent and importance of dCK inhibition in their antiproliferative activity.

ACKNOWLEDGMENT

The authors highly acknowledge the National Plan for Science, Technology and Innovation (MAARIFAH) King Abdulaziz City for Science and Technology—the Kingdom of Saudi Arabia for their financial support under project number (11-MED 1699-10) through Science and Technology Unit (STU) Umm Al Qura University.

CONFLICT OF INTEREST

The authors declare that they have no competing interests.

REFERENCES

[1] U. Pradere, E. C. Garnier-Amblard, S. J. Coats, F. Amblard, R. F. Schinazi, *Chem. Rev.* **2014**, *114*, 9154.
[2] K. Toti, M. Renders, E. Groaz, P. Herdewijn, S. Van Calenbergh, *Chem. Rev.* **2015**, *115*, 13484.
[3] O. Baszczyvnski, Z. Janeba, *Med. Res. Rev.* **2013**, *33*, 1304.
[4] A. Piperno, M. A. Chiacchio, D. Iannazzo, R. Romeo, *Curr. Med. Chem.* **2006**, *13*, 3675.
[5] A. O. Maslat, M. Bkhaitan, G. A. Sheikha, *Drug Chem. Toxicol.* **2007**, *30*, 41.
[6] A. G. M. Sheikha, M. M. Bkhaitan, R. A. Al-Hourani, A. M. Qaisi, R. Loddo, P. La Colla, *Saudi Pharm. J.* **2007**, *15*, 16.
[7] M. Kremerov, in *Herpesviridae – A Look into This Unique Family of Viruses*; In Tech, **2012**.
[8] L. P. Jordheim, D. Durantel, F. Zoulim, C. Dumontet, *Nat. Rev. Drug Discov.* **2013**, *12*, 447.
[9] E. De Clercq, *Annu. Rev. Pharmacol. Toxicol.* **2011**, *51*, 1.
[10] D. G. Piotrowska, M. Cieślak, K. Krõlewska, A. E. Wrõblewski, *Arch. Pharm. (Weinheim).* **2011**, *344*, 301.
[11] U. Chiacchio, E. Balestrieri, B. Macchi, D. Iannazzo, A. Piperno, A. Rescifina, R. Romeo, M. Saglimbeni, M. T. Sciortino, V. Valveri, A. Mastino, G. Romeo, *J. Med. Chem.* **2005**, *48*, 1389.
[12] U. Chiacchio, A. Rescifina, D. Iannazzo, A. Piperno, R. Romeo, L. Borrello, M. T. Sciortino, E. Balestrieri, B. Macchi, A. Mastino, G. Romeo, *J. Med. Chem.* **2007**, *50*, 3747.
[13] A. Piperno, S. V. Giofrè, D. Iannazzo, R. Romeo, G. Romeo, U. Chiacchio, A. Rescifina, D. G. Piotrowska, *J. Org. Chem.* **2010**, *75*, 2798.
[14] E. Balestrieri, C. Matteucci, A. Ascolani, A. Piperno, R. Romeo, G. Romeo, U. Chiacchio, A. Mastino, B. Macchi, *Antimicrob. Agents Chemother.* **2008**, *52*, 54.
[15] U. Chiacchio, D. Iannazzo, A. Piperno, R. Romeo, G. Romeo, A. Rescifina, M. Saglimbeni, *Bioorganic Med. Chem.* **2006**, *14*, 955.
[16] M. F. A. Adamo, R. Pergoli, *Curr. Org. Chem.* **2008**, *12*, 1544.
[17] J. Stambasky, M. Hocek, P. Kocovsky, *Chem. Rev.* **2009**, *109*, 6729.
[18] E. Sabini, S. Ort, C. Monnerjahn, M. Konrad, A. Lavie, *Nat. Struct. Mol. Biol.* **2003**, *10*, 513.
[19] Y. Zhang, J. A. Secrist, S. E. Ealick, *Acta Crystallogr. D Biol. Crystallogr.* **2006**, *62*, 133.
[20] J. Nomme, Z. Li, R. M. Gipson, J. Wang, A. L. Armijo, T. Le, S. Poddar, T. Smith, B. D. Santarsiero, H.-A. Nguyen, J. Czernin, A. N. Alexandrova, M. E. Jung, C. G. Radu, A. Lavie, *J. Med. Chem.* **2014**, *57*, 9480.
[21] A. Matsuda, T. Sasaki, *Cancer Sci.* **2004**, *95*, 105.
[22] H. van de Waterbeemd, E. Gifford, *Nat. Rev. Drug Discov.* **2003**, *2*, 192.
[23] D. F. Veber, S. R. Johnson, H.-Y. Cheng, B. R. Smith, K. W. Ward, K. D. Kopple, *J. Med. Chem.* **2002**, *45*, 2615.
[24] T. I. Oprea, *J. Comput. Aided Mol. Des.* **2000**, *14*, 251.
[25] T. I. Oprea, J. Gottfries, V. Sherbukhin, P. Svensson, T. C. Kühler, *J. Mol. Graph. Model.* **2000**, *18*, 541.
[26] T. Mosmann, *J. Immunol. Methods* **1983**, *65*, 55.
[27] I. Nicoletti, G. Migliorati, M. C. Pagliacci, F. Grignani, C. Riccardi, *J. Immunol. Methods* **1991**, *139*, 271.
[28] A. Gunar, J. Songstad, *Acta Chem. Scand.* **1965**, *19*, 893.
[29] A. Eberhard, F. H. Westheimer, *J. Am. Chem. Soc.* **1965**, *87*, 253.
[30] B. Mochona, X. Qi, S. Euynni, D. Sikazwi, N. Mateeva, K. Soliman, *Bioorg. Med. Chem. Lett.* **2016**, *15*, 1.
[31] E. Sabini, S. Hazra, S. Ort, M. Konrad, A. Lavie, *J. Mol. Biol.* **2008**, *378*, 607.
[32] F. Mao, W. Ni, X. Xu, H. Wang, J. Wang, M. Ji, J. Li, *Molecules* **2016**, *21*, 75.

SUPPORTING INFORMATION

Additional Supporting Information may be found online in the supporting information tab for this article.

How to cite this article: Bkhaitan MM, Mirza AZ, Abdalla AN, et al. Reprofiling of full-length phosphonated carbocyclic 2′-oxa-3′-aza-nucleosides toward antiproliferative agents: Synthesis, antiproliferative activity, and molecular docking study. *Chem Biol Drug Des*. 2017;90:679–689. https://doi.org/10.1111/cbdd.12987